



Research Article

ICONARP
International Journal of Architecture and Planning
Received: 01.10.2020 Accepted: 18.10.2021
Volume 9, Issue 2/ Published: 21.12.2021
DOI: 10.15320/ICONARP.2021.175 E- ISSN:2147-380

ICONARP

Numerical Study of Wind induced Pressures on Irregular Plan Shapes

Tuğba İnan Günaydın¹ 

¹Asst. Prof. Dr., Faculty of Architecture, Niğde Ömer Halisdemir University, Niğde, Turkey. (Principal contact for editorial correspondence), Email: tinan@ohu.edu.tr

Abstract

Purpose

This study researches a numerical analysis of pressure distributions of wind on irregular buildings over wind angles of 0° and 180° with different projection ratios (PR). Wind is an important design parameter that should be considered at the initial part of the design phase in terms of energy potential. For this reason, wind effects in building design is extensively analyzed in this study. The study aims to analyze the effect of irregular building form, projection ratios, the re-entrant corner distances and wind incidence angles on the wind flow and on pressure distributions of wind at all surfaces.

Design/Methodology/Approach

Two L-shaped and T-shaped building models which have the identical building area and building height but have different projection ratios were analyzed by Computational Fluid Dynamics (CFD) of ANSYS. In line with the aim, pressure distributions of wind on and around various irregular buildings are analyzed for the same height level. Model dimensions were reduced to 1/100 scale to save computing time.

Findings

From the study, it has been noticed that the plan shape, projection ratios, distances from the re-entrant corner, considerably influence the wind behavior of buildings. It was noticed that when projection ratio decreased to half, the negative pressure values two times greater in L and T models. When L and T models with the same building area are compared, the highest negative pressure was seen in the L model with the highest projection ratio PR (0.80). In all T models, the highest negative pressure coefficients were noticed on D and F surfaces for both wind angles. In all L models, the highest negative pressure coefficients were found on F surface for both wind angles.

Originality/Value

Studies on the effects of wind on the building are generally seen as an engineering problem. There are limited number of studies on this subject in architecture. However, this is an issue that needs to be investigated, which also concerns architecture. There are many studies in the literature on the wind behavior of irregular buildings. However, projections in plan and distances from the re-entrant corner's effect on pressure coefficients were not be studied comprehensively. The obtained results from the CFD analysis will provide extensive information related to wind effects on buildings. this resource will create awareness about wind for architects and architecture students and can be used as a resource in the design phases.

Keywords: Building form, projections, wind pressure coefficients, computational fluid dynamics

INTRODUCTION

Wind is an important design parameter that should be considered at initial part of the design phase. Understanding the behavior mechanism of buildings under the influence of wind is important in designing our buildings correctly. It is possible to notice a rising interest in analyzing wind load effects on buildings in engineering field.

Wind pressure is a significant design output parameter for analyzing the response of all surfaces of buildings under the wind loads. Wind pressure depends on various factors such as building dimension and shapes, wind incidence angle, built environment and wind characteristics (Xu, Yang, Yoshida, and Tamura (2017); Mou *et al.*, (2017); Zhao and He (2017), 2017; Sy, Yamada, and Katsuchi (2019); Li *et al.*, (2020); Y. He *et al.* (2019).

Mean pressure coefficients are one of the crucial design parameter to perceive wind load effects on buildings. Generally, buildings are organized considering medium pressure coefficients for a curtain surfaces and medium pressure coefficient may vary highly in case of the buildings designed having irregular form. The wind analysis of buildings having irregular forms are extremely complicated due to the complex flow mechanism in irregular formed buildings. Examining the medium wind pressure coefficients on all surfaces of the buildings having irregular plan shaped is significant. Besides, pressure distribution on all surfaces will guide related to wind characteristic of buildings (Bhattacharyya and Dalui (2018); Bairagi and Dalui (2020); Mallick *et al.*, (2020); Liu *et al.*, (2020); Chen *et al.*, (2021), Kummitha *et al.*, (2021); Zhou *et al.*, (2021); Hu *et al.*, (2019); Peng *et al.*, (2020). It has been mentioned in many studies that the effect of pressure distribution is quite complicated in irregular formed buildings. (Bandi *et al.*, 2013); R.Kar and Dalui (2016); Tanaka *et al.*, (2012); Bhattacharyya and Dalui (2020); Liu *et al.* (2020); Sanyal and Dalui (2020)). Mallick *et al.* (2020) analyzed wind behavior of buildings via the corner modifications and various wind angles (Mallick, Kumar, & Patra, 2019). Bhattacharyya and Dalui examined E formed high buildings wind behavior. (Bhattacharyya & Dalui, 2018). Sanyal and Dalui (2021) were analyzed internal corners effects on wind behaviour of Y formed high building. Medium pressures and wind load effects were analyzed in detail for different angle. (Sanyal & Dalui, 2021). Paul and Dalui (2021) analyzed on optimum form for a regular formed high building exposing wind load. They aim to minimize pressure coefficients on all facades. (Paul & Dalui, 2021). Al-Najjar and Al-Azhari (2021) studied wind effects on different formed tall buildings. (Al-Najjar & Al-Azhari, 2021). Bairagi and Dalui (2020) examined pressure variation on a regular and setback high-rise buildings. The authors created the buildings having various setbacks (Bairagi & Dalui, 2020). Jendzelovsky and Antal (2021) investigated on pressure variations on tall buildings for an equilateral acute triangle form with experimentally and numerically (Jendzelovsky & Antal, 2021). The aerodynamic behavior of other irregular forms as E form (Bhattacharyya, Dalui, & Ahuja, 2014) and

C form (Mallick *et al.*, 2019) was evaluated for many wind incidence angle. Pal, Raj, and Anbukumar (2021). Pal *et al.* (2021) investigated on wind behavior of square and fish formed high-rise buildings (Pal *et al.*, 2020). Behera *et al.*,(2020) studied on wind tunnel tests in order to explore the effect of buildings on each other for different ratios in plan. The highest pressure values on windward facade of the main model were examined. It was noticed that the highest pressure coefficients reduced related to the approaching the main model. Tse *et al.*, (2021) examined the corner effects on wind behavior, especially on pressure distributions on surfaces. It was noticed that the decrease in the corner ratios were more effective for minimize the wind behavior. (Tse *et al.*, 2021).

To receive the wind effects on buildings, four methods have been discovered and followed from past to present. These are full-scale measurements, wind tunnel tests, theoretical studies and simulations. However, these field studies are both time-consuming and costly. In recent years, numerical approaches based on computational fluid dynamics (CFD) simulations are being commonly utilized architects for many studies related to understanding the wind behavior. Computational Fluid Dynamics (CFD) method is more economical and commonly accessible compared to the other methods. It provides solving the complex flow conditions via strong mathematical equations (Weerasuriya, 2013). CFD have a significant role in every stage of building design.

Various researches have been realized in order to investigate wind flow and understand wind behavior of buildings. There is considerable study related to regular forms such as square and rectangular building forms. However, there in not more comprehensive studies related on irregular plan shaped buildings.

Ahmad and Kumar (2002) examined the plan shape effect on pressure distributions in low-rise buildings. Gomes *et al.*, (2005) analyzed the L and U formed buildings. They noticed that models present similar behavior for normal wind angle different form the other angles. Kushal *et al.*, (2013) realized that the building form greatly influenced the pressure distributions of wind on all surfaces. Verma *et al.*, (2013) studied the wind angle effects for regular plan formed models. Bhattacharyya *et al.* (2014) examined pressure variations for all surfaces of E formed model for various wind angles. Chakraborty *et al.*, (2014) analyzed of + formed models. They comprised the obtained results from the wind tunnel with simulations. Mukherjee *et al.*, (2014) studied on the effects of wind on Y plan formed high rise buildings via measurements and CFD analysis. The results show a good agreement.

The wind effects on buildings is quite significant in the architectural field that should be perceived. This study presents the CFD analysis for L and T shaped models to examine wind pressure variations for wind angles of 0° and 180°. The aim is to analyze the effect of irregular plan shapes, projection ratios and wind incidence angles on the wind behavior of buildings. Wind pressure distributions on all surfaces for L and T formed

models are studied in detail over the wind angle of 0° and 180° . This research intends to explore the wind effects on buildings having different irregular plan geometries. Two L and T shaped buildings were designed to have the same height and building area. The models having different projection ratios were analyzed by CFD of ANSYS. From the analysis, wind pressure variations on and around various irregular formed models are examined. The obtained comprehensive results from the CFD analysis will provide extensive information related to wind effects on and around buildings. Architects and architectural students can utilize from the results at the beginning of the design stage.

METHODOLOGY

To design numerical models properly and provide reliable findings, various parameters must be taken into account. The significant ones are computational domain, meshing, boundary conditions, solver settings, and control of residuals. If parameters are not well considered, the analysis represent unrealistic results. ANSYS FLUENT 20.0 software is used in this research. Computational Fluid Dynamics (CFD) e of is used for the analysis. In recent years, the use of numerical analysis has become widespread by ANSYS-FLUENT among architects and engineers.

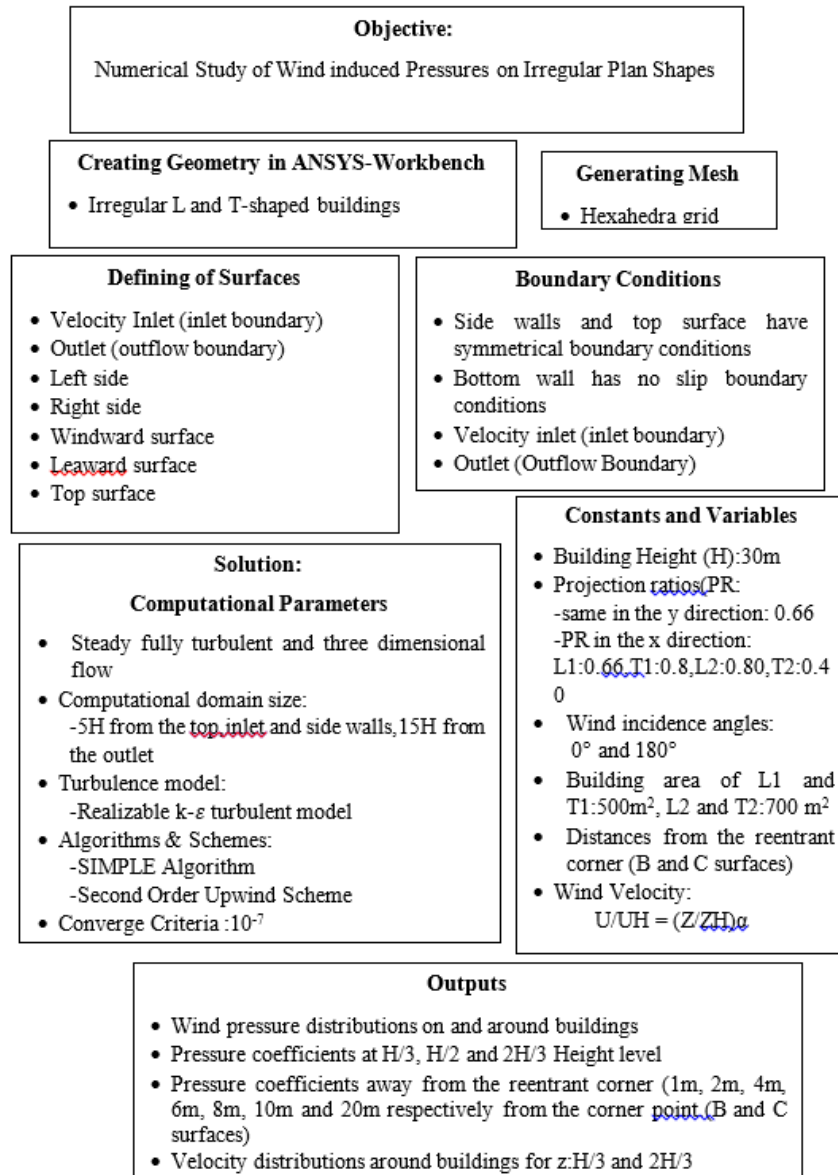
In this study model dimensions were reduced to 1/100 scale to save computing time. CFD analysis consist of three part as computational domain, meshing and boundary conditions The process of the research is presented in Table 1. Each step of the research is presented comprehensively.

Computational Domain and Meshing

The computational area must be large enough to avoid reflection of fluid flows that can create extreme pressure zones around the buildings (Franke, 2006). Also, the distances around the models should be distant enough in order to allow the wind flow improvement. (He *et al.*, 2014).

Huang *et al.*, (2005) displayed the computational domains for high-rise single models. The distance between the top of model and computational domain and the distance from the inlet should be at least 5H. H is building height. Besides, side distances of computational domain are 2 to 3 times greater than the building width (W). Besides, the distance between the back side of the building and outlet boundary is proposed minimum 15H (Franke, 2006). Tominaga *et al.* (2008) proposed 5H for side boundaries and inlet and minimum 10H from the outlet (Tominaga *et al.*, 2008). Designing the computational domain correctly is considerably significant in terms of obtaining reliable results (Blocke *et al.*, 2007).

Table 1. Flowchart of the study



In this research, the distance is 5H from the sides, inlet and top surfaces. Also, the distance from the outlet is 15H (Figure 1). The used grid type is a hexahedra grid. The maximum skewness values, mesh quality and other parameters for the prediction are provided. Model dimensions were reduced to 1/100 scale to save computing time. The position of model in computational domain is shown in Figure. 1.

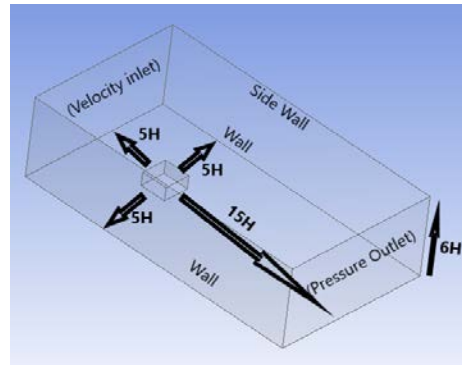


Figure 1. Computational Domain

Boundary Conditions

Boundary conditions are considerably significant on solutions inside the computational domain. Therefore, they should be chosen properly for the reliable results in numerical simulations (Franke, 2006). Inlet, outlet, side and top surfaces boundary conditions are considerably significant. In this research, inlet boundary is assumed as velocity inlet. Side and top surfaces assumed as having symmetric boundary conditions. Besides, ground has no-slip. The chosen turbulent model is realizable $k-\varepsilon$ for the analysis.

Boundary layer wind flow near the windward surface was created in the inlet of the domain utilizing power law:

$$U/U_H = (Z/Z_H)^\alpha \dots \dots \dots (1)$$

Where U is the horizontal wind velocity at an elevation Z ; U_H is the velocity at the reference elevation Z_H (10 m/s); Z_H is the boundary layer height (1.0 m) and α is power law index (0.133).

For solving the pressure-velocity coupling, SIMPLE algorithm of Patankar was used (Patankar, 1980). Moreover, Second-Order Upwind Scheme was driven for the terms convection and viscous terms. In the study, the convergence criterion was assumed as 10^{-7} .

Models

Two L and T formed models designed as having the same plan area and height but having different projections in plan. Wind pressure coefficients were analyzed numerically on irregular formed building models over wind incidence angles of 0° and 180° . The aim is to analyze the effect of plan shape, the reentrant corner, projection ratio of wing and wind incidence angles on the wind behavior on buildings. Models could be categorized according to building form and their dimensions including projection ratio of wing (PR) ratio according to both x and y direction. Information about the models is given in Figure 2 and Table 2 in detail. Projection value (PR) is calculated for both x and y direction. It is assumed as the ratio of the wing to the whole length. All of the models have same projection ratio of 0.66 on y direction. The surfaces on models were denoted with letters as presented in Figure 2. All of the models have projection irregularity in plan which is coded A3 irregularity in the

Turkish Earthquake code. They are all designed as having a building height of 30 m. While the model L1 and T1 have the same building area of 500 m², the model L2 and T2 have the same building area of 700 m².

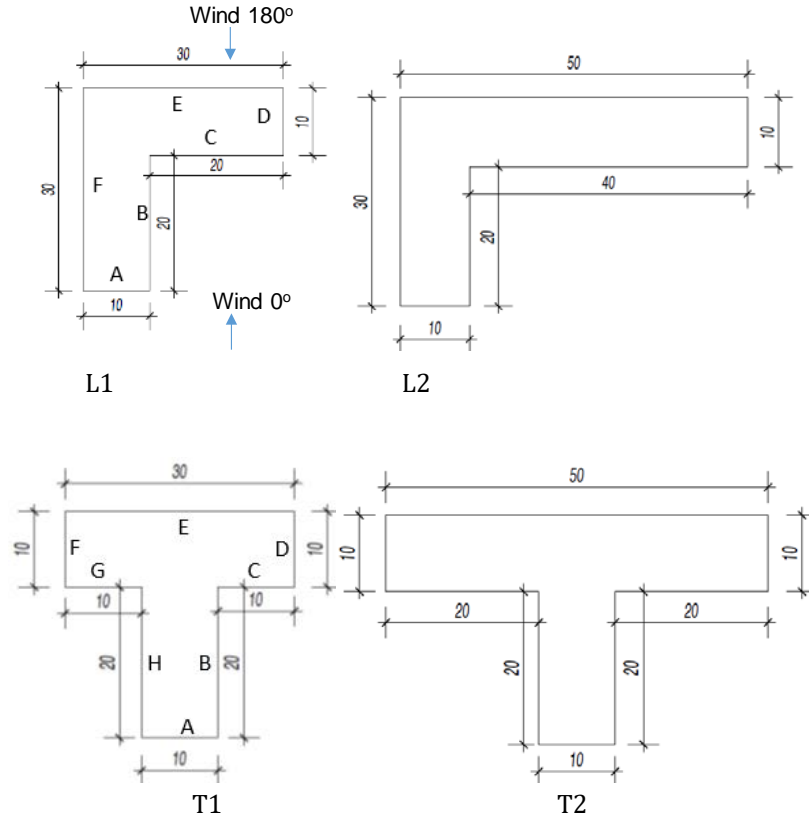
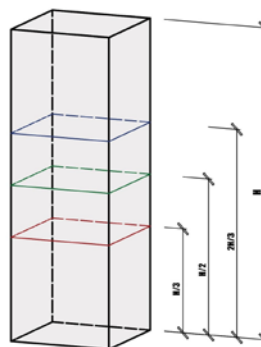


Figure 2. Building models

Table 2. Projections and computational domain information

Model	PR1	PR2	Computational Domain (m) X x Y x Z
	(x)	(y)	
L1	0.66	0.66	330 x 180 x 630
L2	0.80	0.66	350 x 180 x 630
T1	0.33	0.66	330 x 180 x 630
T2	0.4	0.66	350 x 180 x 630

Figure 3. Horizontal lines for pressure coefficients



To examine wind characteristics of on L and T plan-shaped models, pressure coefficients are sliced at the height level of $2H/3$, $H/2$ and $H/3$, as presented symbolically in a simple square form on Figure 3. Another important point investigated in the study is the changes in the pressure coefficients as they move away from the reentrant corner points. Therefore, vertical lines are created on B and C surfaces. These lines are at a distance of 10mm, 20mm, 40mm, 60 mm, 80 mm and 100mm respectively from the corner point according to 1/100 scale (Figure 4).

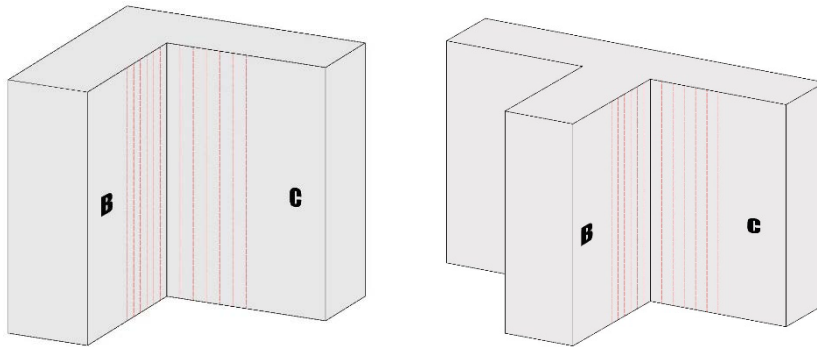


Figure 4. Vertical lines position

RESULTS AND DISCUSSION

In the study, wind pressure and velocity variations on and around for L and U formed models were analyzed in detail based on the changes in projection ratios, building areas, distances from reentrant corners and height levels. The obtained findings from the CFD simulations is analyzed comprehensively in this section.

Variations on Pressure Coefficients at Model Surfaces

The variations on pressure coefficients were analyzed compressively for all surfaces of all models. The models have the same projection ratios on Y direction. However, they have different projection ratios on X direction. All models were analyzed for wind incidence angle of 0° and 180° . The distribution of pressure coefficients on the surfaces of models were presented in Table 3-4.

The model denoted as L1 is a 30 m irregular building having a L plan shaped and it has a projection ratio (PR) of 0.66 on both X and Y direction. Wind pressure coefficient distributions on L1 plan shape building model over wind incidence angles of 0° and 180° are illustrated in Figure 5-6.

In L1 and L2 model with an incidence angle of 0° , the surfaces coded as A and C exposed to pushing forces and take positive pressure coefficients. A and C surfaces can be called as a windward surface. On the other hand, leeward and side surfaces take negative pressure coefficients. The surface coded as E behave like a leeward surface and F and D the side surfaces for incidence angle of 0° .

In L1 and L2 model with an incidence angle of 180° , the surface E is windward surface and take positive pressure coefficients. However, negative pressures are observed on E surface nearest to side surfaces

both D and F surface and on the top surface. All the other surfaces take negative pressure coefficients.

Table 3. The highest and lowest pressure coefficients for all surfaces of all models for wind incidence angle of 0°

		L1		L2			
		$PR_x :0.66,$ $PR_y:0.66$ Area:500m ²				$PR_x :0.80,$ $PR_y:0.66$ Area:700m ²	
		max. cp (+)	max. cp (-)	max. cp (+)	max. cp (-)		
A		0.767	-0.543	0.778	-0.600		
B		0.657	-0.576	0.683	-0.771		
C		0.707	-0.676	0.700	-0.824		
D		-	-0.705	-	-0.737		
E		-	-0.452	-	-0.511		
F		-	-1.107	-	-1.234		

		T1		T2			
		$PR_x :0.33,$ $PR_y:0.66$ Area:500m ²				$PR_x :0.40,$ $PR_y:0.66$ Area:700m ²	
		max. cp (+)	max. cp (-)	max. cp (+)	max. cp (-)		
A		0.894	-	0.869	-		
B		0.225	-0.226	0.413	-0.288		
C		0.500	-0.182	0.777	-0.288		
D		0.368	-0.677	0.188	-0.794		
E		-	-0.296	-	-0.384		
F		0.360	-0.673	0.177	-0.787		
G		0.490	-0.108	0.776	-0.301		
H		0.229	-0.216	0.417	-0.301		

In L1 model for the incidence angle of 0°, the surface A behaves windward surface and take positive pressure coefficients. However, negative pressures are observed on A surface nearest to the F surface and on top surface. This is similar in L2 model. While, maximum positive pressure coefficient on the surface A of L1 model was 0.767, absolute value of maximum negative pressure was 0.543. B surface expose to both positive and negative forces. Negative forces were observed on the top of the L1 model nearest to the reentrant corner. Besides, higher positive pressure coefficients were observed nearest to the surface C. It is similar in L2 model. While, maximum positive pressure coefficient was 0.657 on the B surface, absolute value of maximum negative pressure was 0.576. C surface behave like a windward surface. However, negative pressure

coefficients are observed on the C surface nearest to D surface and on top surface. This condition is similar with L2 model. On the C surface, maximum positive pressure coefficient was 0.707, the absolute value of maximum negative pressure was 0.676. D and F surfaces are side surfaces and they are directly under negative pressure. While the maximum absolute negative pressure coefficient was 0.705 on D surface, it was 1.107 on F surface. E was the leeward surface and expose to negative pressure. On the E surface, maximum negative pressure was 0.452.

In L1 model for the incidence angle of 0°, negative pressure coefficients on side surfaces (F and D) are higher than the leeward surface (E). The greatest negative pressure coefficients were observed on surface F (1.107). Besides, the maximum positive pressure coefficient was observed on the A surface (0.767).

Table 4. The highest and lowest pressure coefficients for all surfaces of all models for wind incidence angle of 180°

	L1			L2	
	max. cp (+)	max. cp (-)		max. cp (+)	max. cp (-)
	 $PR_x:0.66, PR_y:0.66$ Area:500m ²		 $PR_x:0.80, PR_y:0.66$ Area:700m ²		
A	-	-0.400	A	-	-
B	-	-0.342	B	-	0.439
C	-	-0.342	C	-	0.388
D	-	-0.654	D	-	0.388
E	0.727	-0.544	E	0.733	-
F	-	-1.069	F	-	0.694
				-	1.249
<hr/>					
	T1			T2	
	max. cp (+)	max. cp (-)		max. cp (+)	max. cp (-)
	 $PR_x:0.33, PR_y:0.66$ Area:500m ²		 $PR_x:0.40, PR_y:0.66$ Area:700m ²		
A	-	-0.252	A	-	-
B	-	-0.334	B	-	0.306
C	-	-0.334	C	-	0.367
				-	0.367

D	0.094	-0.770	D	0.06	-
				7	0.81
					2
E	0.769	-0.141	E	0.73	-
				4	0.25
					5
F	0.107	-0.766	F	0.06	-
				8	0.79
					2
G	-	-0.329	G	-	-
					0.37
					4
H	-	-0.328	H	-	-
					0.36
					5

In L1 model for the incidence angle of 180° , the surface E is windward surface and take positive pressure coefficients. However, negative pressures are observed on E surface nearest to side surfaces both D and F surface and on the top surface. All the other surfaces take negative pressure coefficients. The maximum absolute negative pressure coefficient on surface A was 0.400. B and C surfaces showed similar behavior. The maximum absolute value of pressure coefficient was 0.342 on both B and C surfaces. The maximum absolute negative pressure coefficient was 0.654 on the D surface. Also, E surface showed the greatest positive pressure coefficient was 0.727. Besides, the greatest absolute negative pressure coefficient was 0.544 on that surface. Moreover, in L1 model for incidence angle of 180° the greatest negative pressure coefficient was 1.069 on the surface F.

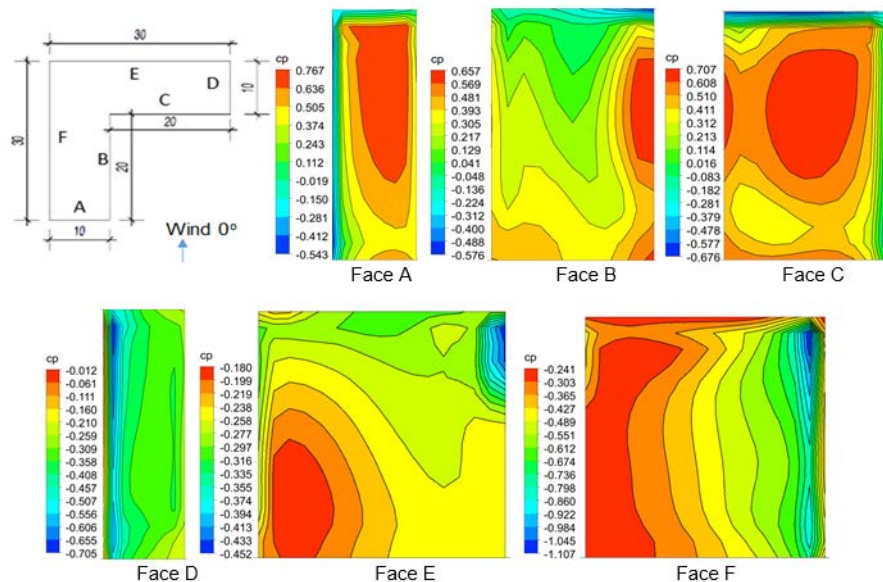


Figure 5. Mean Pressure coefficients in Model L1 for 0° wind incidence angle

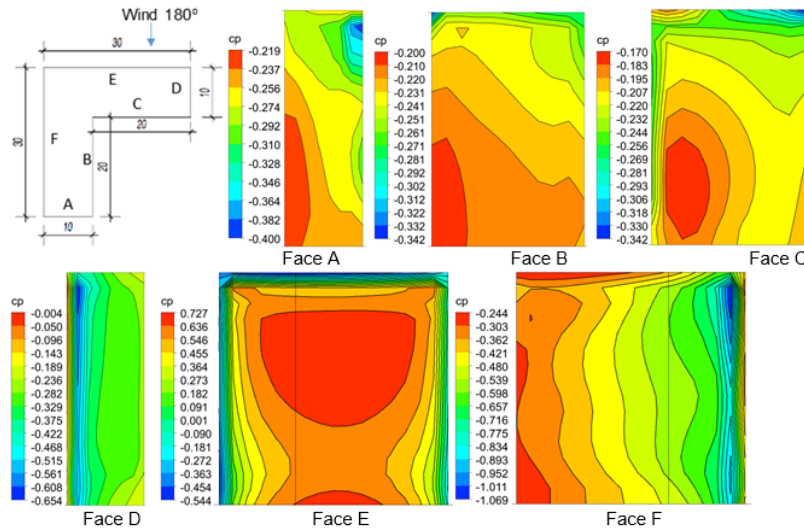


Figure 6. Mean Pressure coefficients in Model L1 for 180° wind incidence angle

While, maximum positive pressure coefficient on the surface A of L2 model was 0.778, greatest pressure coefficient was 0.600. On B surface, maximum positive pressure coefficient was 0.683 and greatest negative pressure was 0.771. On C surface, greatest positive pressure coefficient was 0.700 and the greatest negative pressure was 0.824. While the greatest negative pressure coefficient was 0.737 on D surface, it was 1.234 on F surface. On the E surface, the greatest negative pressure was 0.511.

For L2 model for the incidence angle of 0°, Negative pressure values on the side surfaces (F and D) are higher than negative pressure values on the leeward surface (E). Moreover, Surface C displays more critical negative pressure coefficients than the E surface. The greatest negative pressures coefficients were observed on surface F (1.234). Besides, the maximum positive pressure coefficient was observed on the A surface (0.778).

In L2 model for wind angle of 180°, the maximum negative pressure coefficient on surface A was 0.439. B and C surfaces showed similar behavior. The greatest pressure coefficient was 0.388 on both B and C surfaces. The greatest negative pressure coefficient was 0.731 on D surface. Also, E surface which was the windward surface, showed the greatest positive pressure coefficient was 0.733. Besides, the greatest negative pressure coefficient was 0.694 on that surface. Moreover, the greatest negative pressure coefficient was 1.249 on surface F. (Figure 7-8).

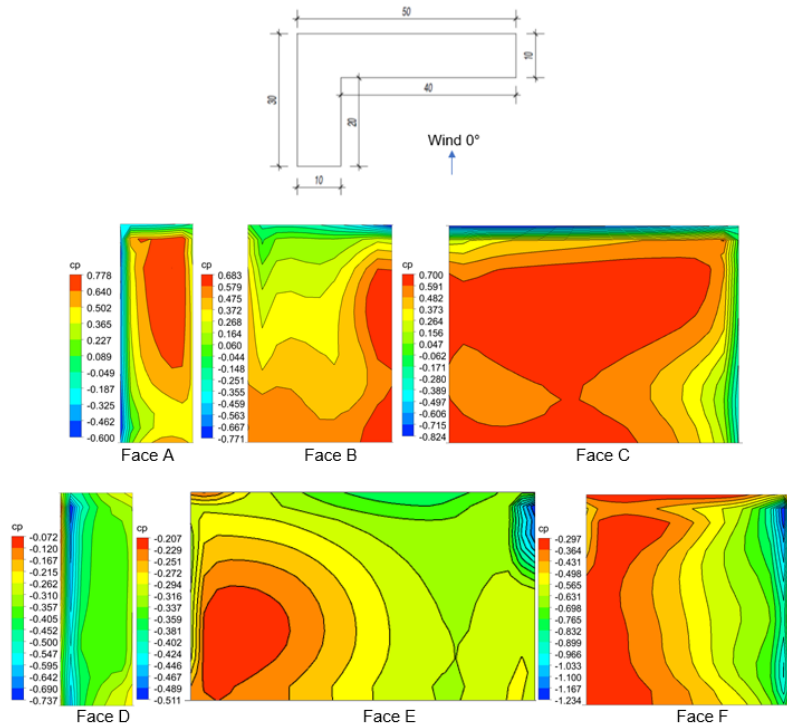


Figure 7. Mean Pressure coefficients in Model L2 for 0° wind incidence angle

In T1 and T2 model with an incidence angle of 0°, the surfaces coded as A, G and C exposed to pushing forces and take positive pressure coefficients. In that condition, A, G and C surfaces behave like a windward surface. On the other hand, negative pressure coefficients were observed in all surfaces except A surface, and positive pressure coefficients are noticed except E surface. E is the leeward surface for 0°wind angle.

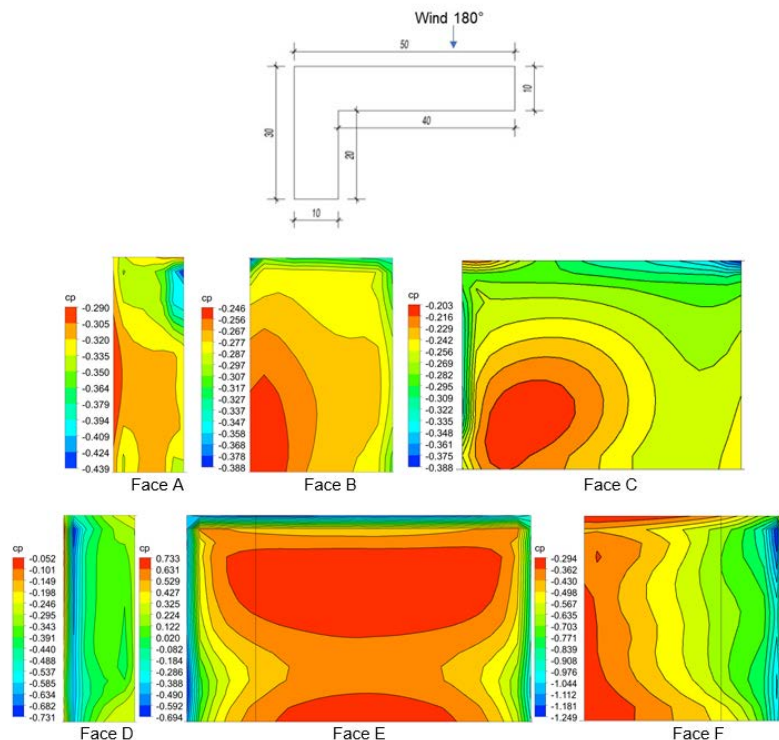


Figure 8. Mean Pressure coefficients in Model L2 for 180° wind incidence angle

In T1 and T2 model with an incidence angle of 180° , the surface E is windward surface and take positive pressure coefficients. However, negative pressures are observed on E surface nearest to side surfaces both D and F surfaces. Positive pressure values are observed at a small value in the regions of the D and F surfaces close to the G and C surfaces. All the surfaces take negative pressure coefficients.

In T1 model for the incidence angle of 0° , maximum positive pressure coefficient on surface A was 0.894. It did not have negative pressure coefficient. All the other surfaces have both positive and negative pressure coefficients. B and H surfaces expose to both positive and negative forces and these values are similar. While, greatest positive pressure coefficient was 0.229 on H surface, greatest negative pressure was 0.226. On C and G surfaces, greatest positive pressure coefficient was 0.500 and the greatest negative pressure coefficient was 0.182. D and F surfaces are side surfaces. While the greatest negative pressure coefficient was 0.677, the maximum positive pressure coefficient was 0.368 on that surfaces. E was the leeward surface and expose to negative pressure. The greatest negative pressure coefficient was 0.296 on E surface.

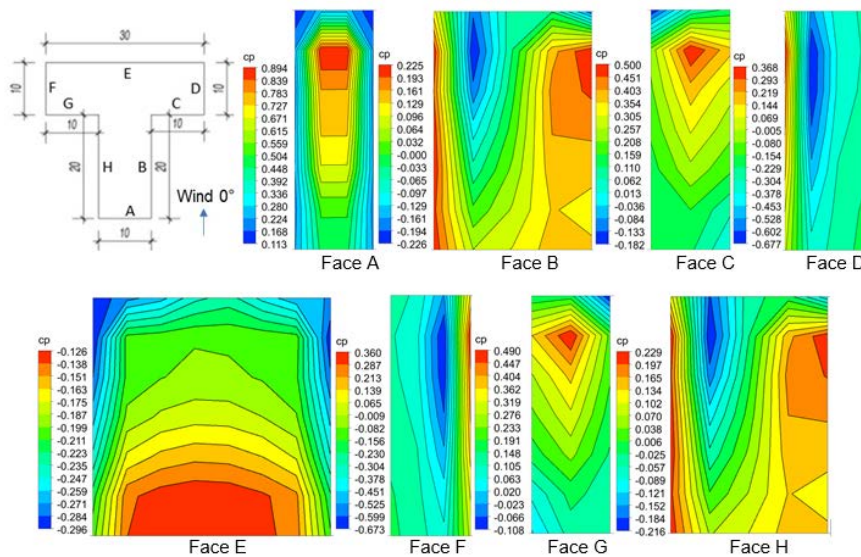


Figure 9. Mean Pressure coefficients in Model T1 for 0° wind incidence angle

In T1 model for the incidence angle of 180° , the surface E is windward surface and take positive pressure coefficients. However, negative pressures are observed on E surface nearest to side surfaces both D and F surface. Besides, D and F, the side surfaces take both positive and negative pressure coefficients. All the other surfaces take negative pressure coefficients. The highest negative pressure coefficient on surface A was 0.252. B and C surfaces and G and H surfaces showed similar behavior. The maximum absolute value of pressure coefficient was 0.334 on that surfaces. The maximum absolute negative pressure coefficient was 0.770 on the side surfaces of D and F surface. The greatest

negative pressure coefficients were observed on D and F surfaces. Also, the E surface which was the windward surface, showed the highest positive pressure coefficient was 0.769. Besides, the greatest negative pressure coefficient was 0.141 on that surface. (Figure 9-10).

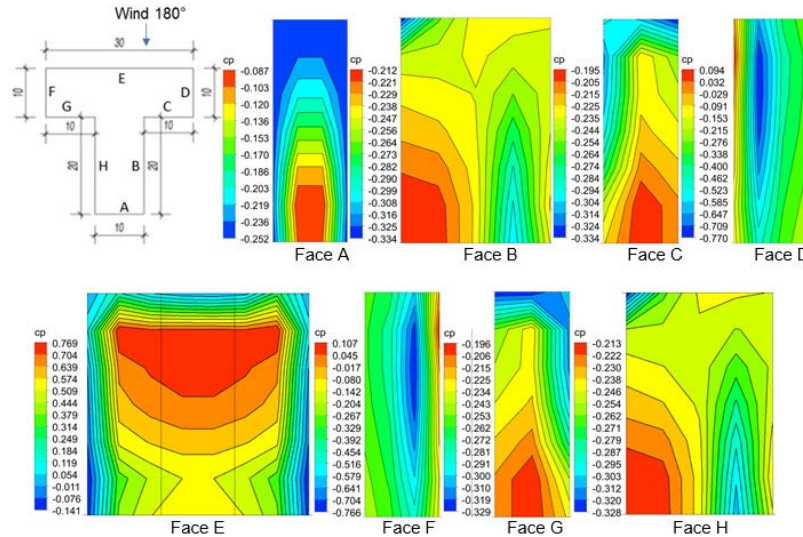


Figure 10. Mean Pressure coefficients in Model T1 for 180° wind incidence angle

In T2 model for the incidence angle of 0°, maximum positive pressure coefficient on the surface A was 0.869. It did not have negative pressure coefficient. All the other surfaces have both positive and negative pressure coefficients except E surface. It shows only negative pressures. B and H surfaces expose to both positive and negative forces and these values are similar. While, highest positive pressure coefficient was 0.417 on the H surface, the highest negative pressure was 0.301. The highest positive pressure coefficient was 0.777, negative pressure coefficient was 0.301 on C and G surfaces. D and F surfaces are side surfaces. While the greatest negative pressure coefficient was 0.794, the maximum positive pressure coefficient was 0.188 on that surfaces. E was the leeward surface and expose to negative pressure. On the E surface, the absolute value of maximum negative pressure was 0.384.

In T2 model for the incidence angle of 180°, the surface E is windward surface and take positive pressure coefficients. However, negative pressures are observed on E surface nearest to side surfaces both D and F surface. Besides, D and F the side surfaces take both positive and negative pressure coefficients. All other surfaces take negative pressure coefficients. The greatest negative pressure coefficient on surface A was 0.306. B and C surfaces and G and H surfaces showed similar behavior. The highest pressure coefficient was 0.374 on that surfaces. The highest negative pressure coefficient was 0.812 on the side surfaces of D and F surface. The greatest negative pressure coefficients were observed on D and F surfaces. On the other hand, the E surface which was the windward surface, showed the highest positive pressure coefficient was 0.734

Besides, the greatest absolute value of negative pressure coefficient was 0.255 on that surface. (Figure 11-12).

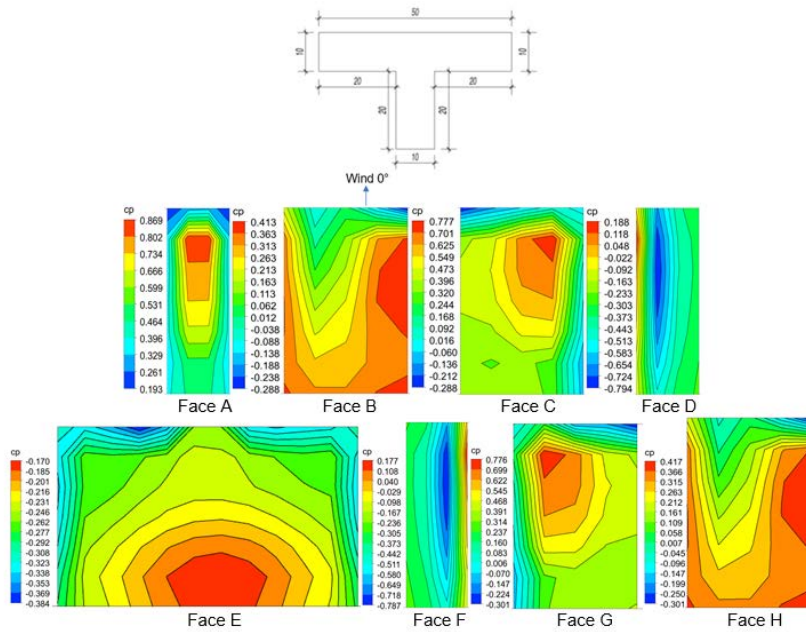


Figure 11. Mean Pressure coefficients in Model T2 for 0° wind incidence angle

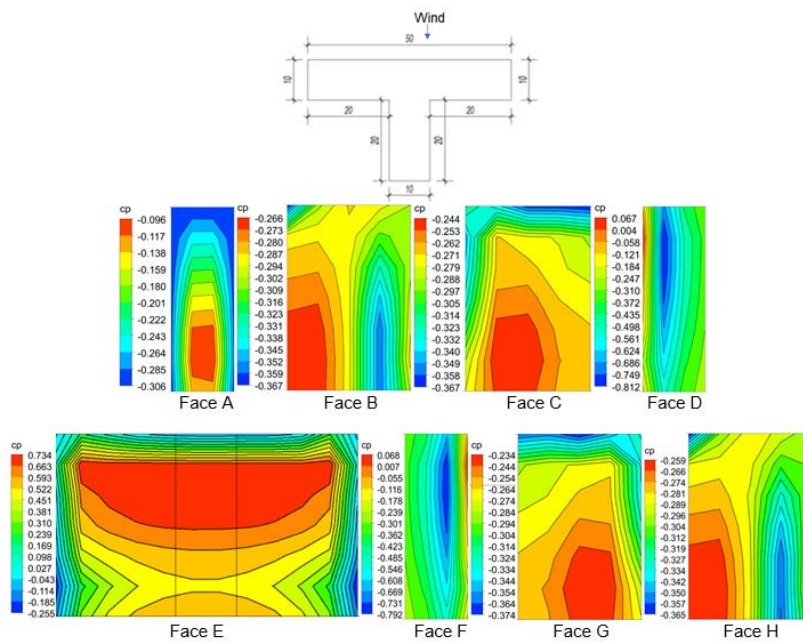


Figure 12. Mean Pressure coefficients in Model T2 for 180° wind incidence angle

To summarize the obtained significant results, when L1 and L2 models were compared, elongation of the surface C, or in other words, the increase of the projection ratio from 0.66 to 0.80, the positive and negative pressure coefficients increased in all L-shaped models for both 0° and 180° wind incidence angle. These increases are more noticeable in negative pressures rather than positive pressures. Moreover, these negative pressure coefficient increases are more clearly observed on B, C and F surfaces in L models where the wind angle is 0°. On the other hand,

in L models where the wind angle is 180 degrees, these negative pressure coefficient increases are more clearly seen on the D, E and F surfaces. In both cases where the wind angle is 0 degrees and 180 degrees, the maximum negative pressure in all L models is on the F surface. Moreover, In L models, the highest negative pressure was recorded on the F surface when the wind angle was 180 degrees as 1.249. When the wind angle is 180 degrees, similar negative pressures are noticed on the B and C surfaces on both L 1 and L2 model. Besides, in the case where the wind angle is 0 degrees, a significant increase in negative pressure coefficients was observed on C surface in L2 model compared to the L1 model. In other words, the increase in the projection ration caused a rise in the negative pressure coefficient on the C surface. On the other hand, when we look at windward surfaces in L1 and L2 models, when the wind angle is 0 degrees, total positive pressure coefficients on A and C surfaces is considerably higher than the E surface when the wind angle is 180 degrees.

In T models for 0° wind incidence angle, with elongation of the surface C and G, or in other words, the increase of the projection ratio from 0.33 to 0.40 in the line of X direction, while the positive and negative pressure coefficients on the B, C, G and H surfaces rise, the positive pressure coefficients on the D and F surfaces decrease significantly. However, negative pressure values increased on D and F surfaces. In addition, a slight decrease was observed in the positive pressure coefficient on the A surface. Moreover, as the E surface got longer, the negative pressure coefficient on its surface increased. With elongation of the surfaces C and G, all negative and positive pressure coefficients increased. In T models for 180° wind incidence angle, with elongation of the surfaces C and G, while the positive pressure coefficients on the D, E and F surfaces decrease, the negative pressure coefficients increase. In shortly, with elongation of the surfaces C and G, while all positive pressure coefficients decreased, all negative pressure coefficients increased in T models for 180° wind incidence angle. Besides, in T models for 0° wind incidence angle, while all negative pressure coefficients increased, positive pressure coefficients increased except A, D and F surfaces. When we look at windward surfaces in T1 and T2 models, when the wind angle is 0°, total positive pressure on A, C and G surfaces is considerably higher than the E surface when the wind angle is 180 degrees. While the highest positive pressure coefficient was observed in T1 model for 0° wind incidence angle, the highest negative pressure coefficient was noticed in T2 model for 180° wind incidence angle.

Pressure coefficients on horizontal lines

The surfaces are sliced respectively at $2H/3$, $H/2$, and $H/3$ height level were given in Figure 3. In Figure 13, the C_p values of all surfaces were given for L1 model for the incidence angle of 0° and 180°. In L1 model for the of 0° wind incidence angle, c_p coefficients on windward surfaces (A and C surface) increased along the height of the building. Moreover, on

leeward surface (E surface) and the side surfaces (D and F surface), c_p coefficients increased slightly along the height of the building. On the contrary, c_p coefficients on B surface tend to decrease along the height of the building. However, these coefficients tend to increase as they near to the windward surfaces of the surface of A and C. In L1 model for the of 180° wind incidence angle, all c_p coefficients increased in all surfaces as the building height increased. Moreover, this increase is clearly observed in the E surface.

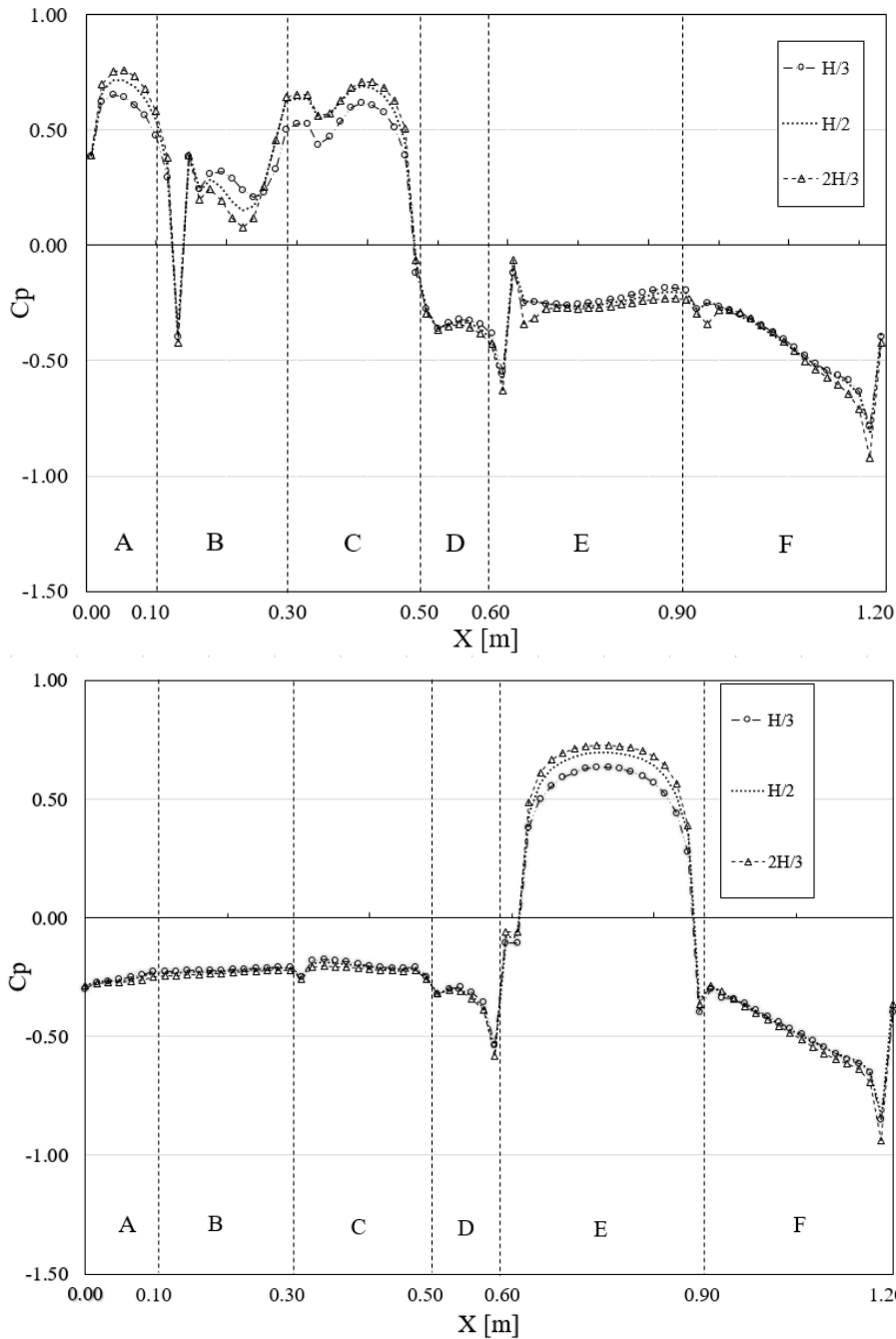


Figure 13. Pressure coefficients of L1 model along the horizontal lines for 0° and 180° wind incidence angle, respectively

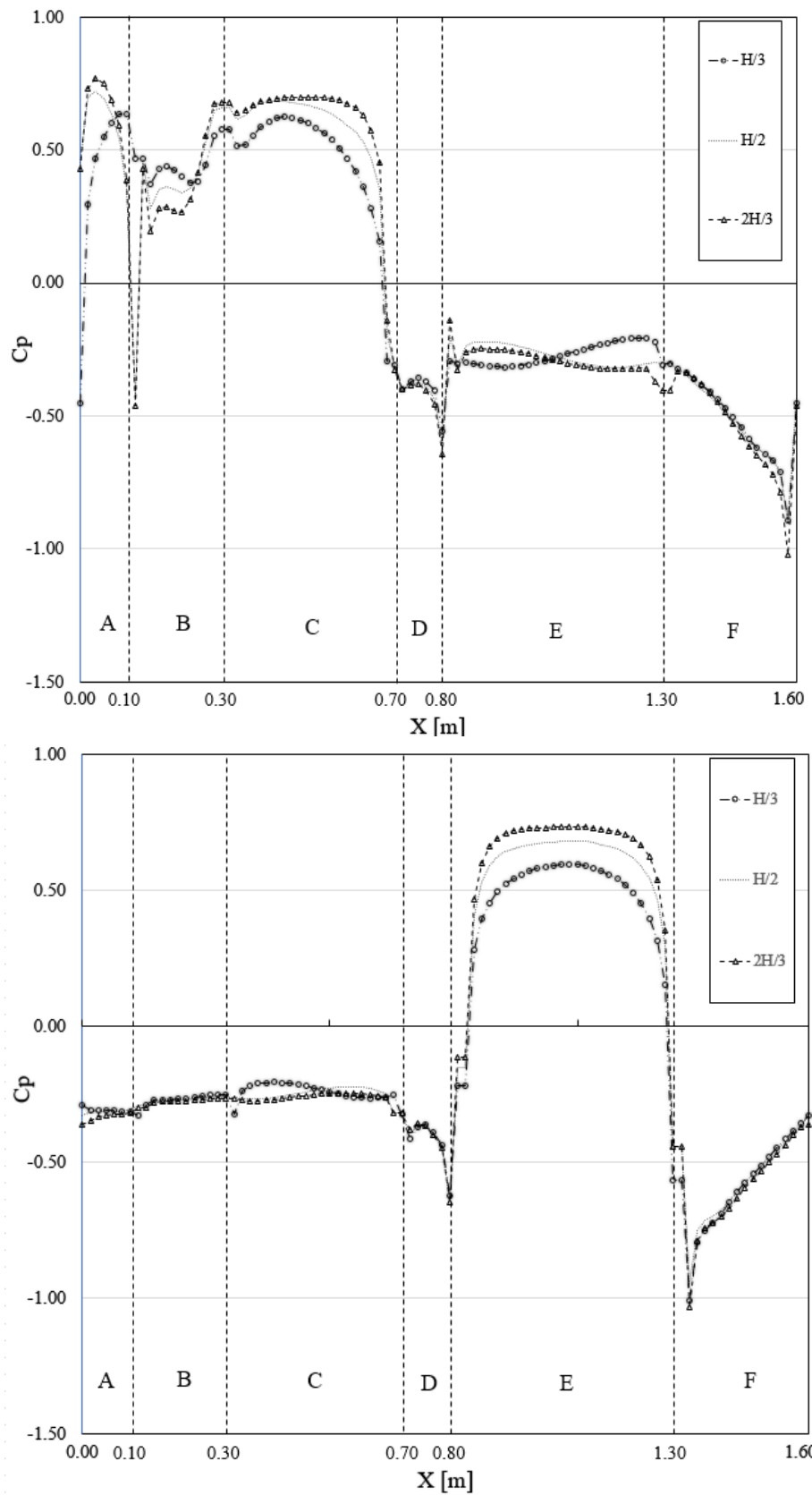


Figure 14. Pressure coefficients of L2 model along the horizontal lines for 0° and 180° wind incidence angle, respectively

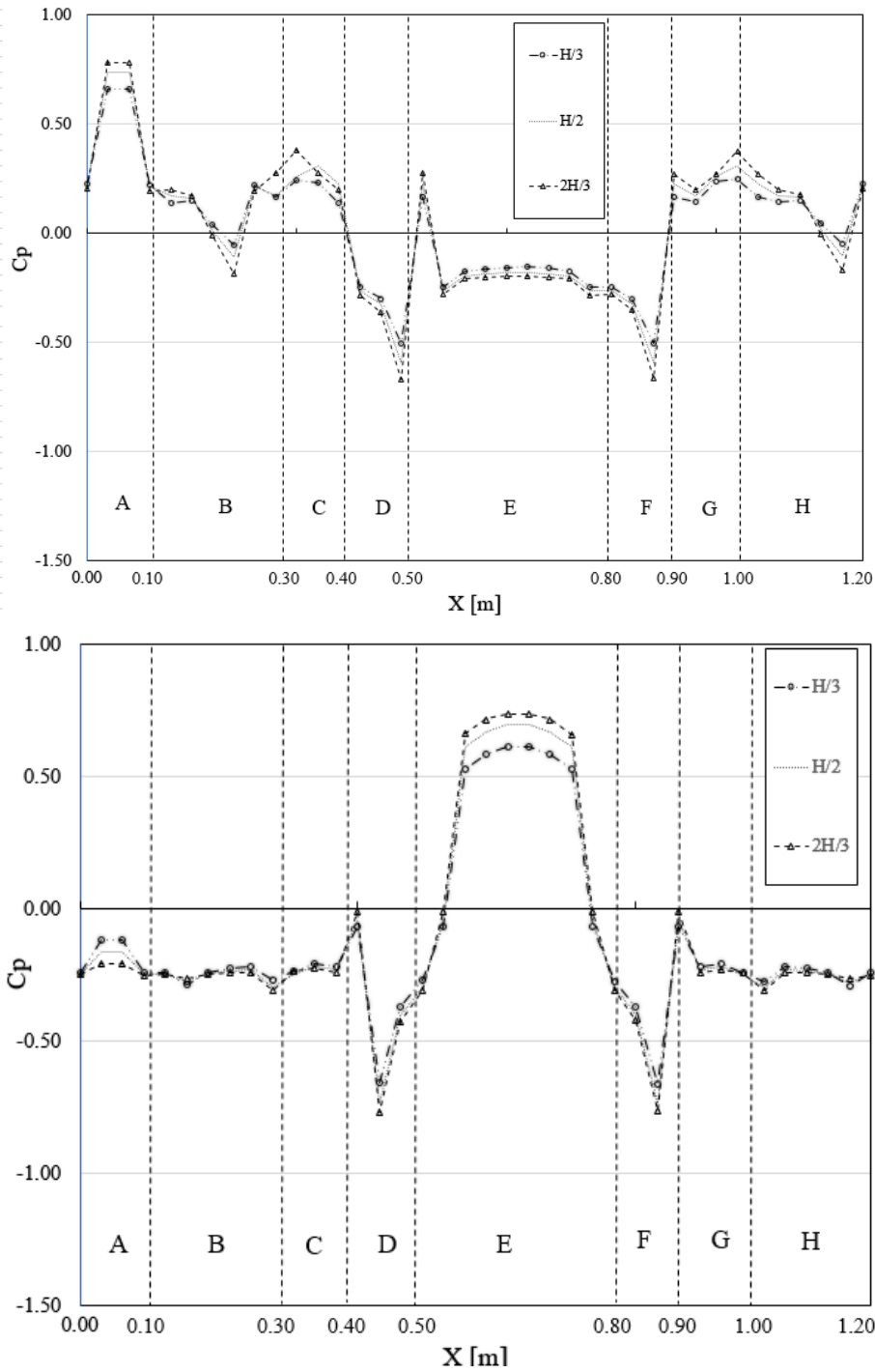


Figure 15. Pressure coefficients of T1 model along the horizontal lines for 0° and 180° wind incidence angle, respectively

In Figure 14, the C_p values of all surfaces were given for L2 model for the incidence angle of 0° and 180°. In L2 model for the 0° wind incidence angle, c_p coefficients on windward surfaces (A and C surface) increased along the height of the building. Moreover, on leeward surface (E surface) and the side surfaces (D and F surface), c_p coefficients increased slightly along the height of the building. On the contrary, c_p coefficients on B surface tend to decrease along the height of the building. However, these coefficients tend to increase as they near to the windward surfaces of the surface of A and C. In L2 model for the of 180° wind incidence angle, all c_p

coefficients increased in all surfaces as the building height increased. Moreover, this increase is clearly observed in the E surface.

In Figure 15, the C_p values of all surfaces were given for T1 model for the incidence angle of 0° and 180° . In T1 model for the 0° wind incidence angle, while a regular increase or decrease was not observed in the pressure coefficients on B,D,F and H surfaces, it was noticed that the pressure coefficients increased with height of the building on all other surfaces. All these features are similar to the T1 model for the 180° wind incidence angle. However, the rise in pressure coefficients is clearly observed in A and E surfaces for the 180° wind incidence angle (windward and leeward surfaces, respectively).

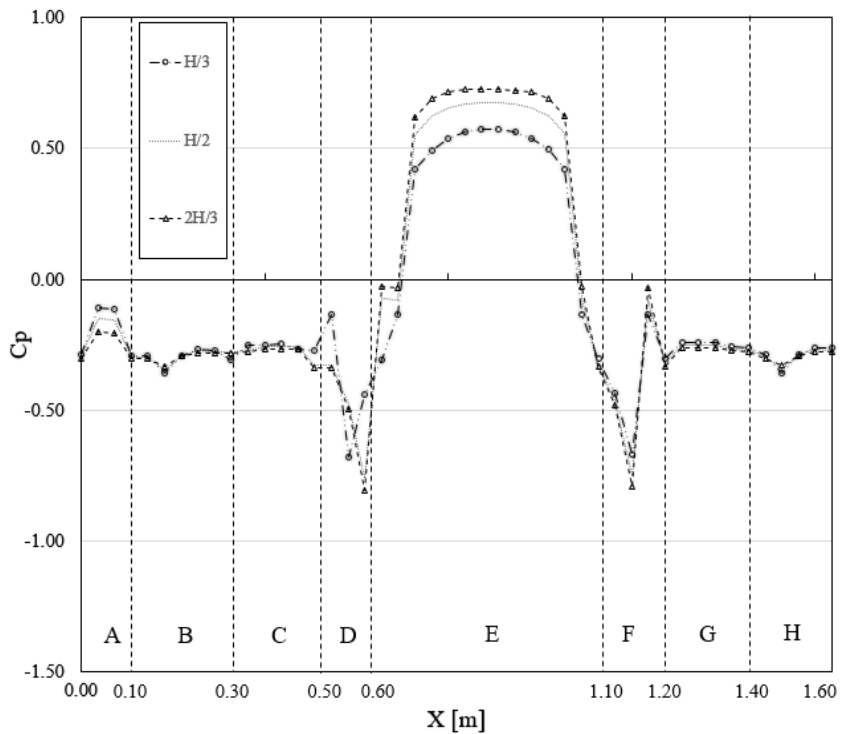
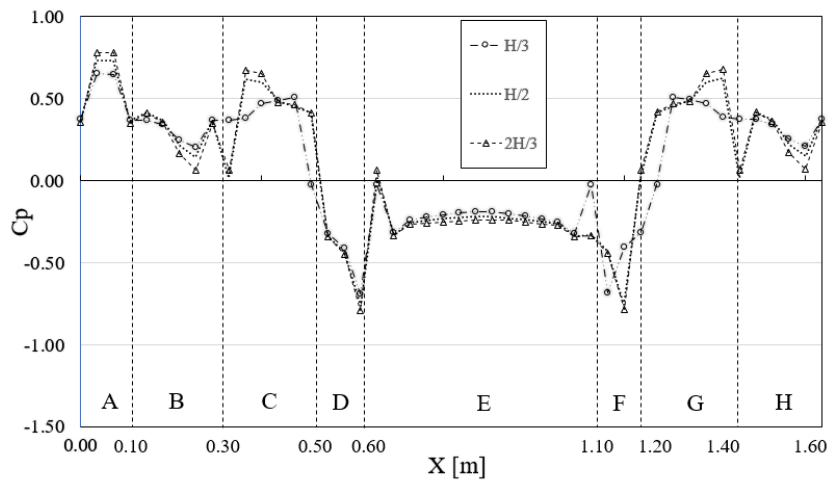


Figure 16. Pressure coefficients of T2 model along the horizontal lines for 0° and 180° wind incidence angle, respectively

In Figure 16, the C_p values of all surfaces were given for T2 model for the incidence angle of 0° and 180° . In T2 model for the 0° wind angle, the increase in the pressure coefficients is clearly observed in A and E surfaces (windward and leeward surfaces, respectively). There was no a regular increase or decrease on the other surfaces. In T2 model for 180° wind incidence angle, the pressure coefficients tend to increase along the building height except surfaces of D and F. Moreover, the rise in the pressure coefficients is clearly observed in A and E surfaces for the 180° wind incidence angle (windward and leeward surfaces, respectively).

Pressure coefficients on vertical lines

The changes on pressure coefficient on the vertical lines designed at different distances from the corner of the building are shown in Figure 17 on the L1 formed models for the situation where the wind comes at an angle of 0° . It has been noticed that the pressure coefficients decrease on B surface as the vertical lines move away from the corner point of the building. Furthermore, the pressure coefficients on all vertical lines decrease approximately to 5 meters of the building height, then increase to 20 meters of the building and then decrease again and negative pressure coefficients are noticed following 25th meter. The highest positive and negative pressure values were noticed on the line 1 meter away from the reentrant corner on the B surface. These highest pressure coefficients are 0.65 and -0.57. Also, for L1 model, a regular increase or decrease were not observed on the pressure coefficients on C surface, as the distance between vertical lines and re-entrant corner increase. The highest positive and negative pressure coefficients on surface C were noticed on the vertical lines nearest to the middle of the C surface. The highest ones were noticed on vertical line which is 10 meter distance from the re-entrant corner. In other words, the highest pressure coefficients were observed on the vertical line in the middle of the C surface. The highest positive and negative pressure coefficients are 0.70 and -0.67, respectively. Moreover, the behavior of the pressure coefficients across the building height is similar to that on the B surface. The changes on pressure coefficient on the vertical lines are shown in Figure 18 on the L2 formed models for the situation where the wind comes at an angle of 0° . On B surface, as the distance between vertical lines and the re-entrant corner increase, the pressure coefficients decreased as similar to surface B of L2-shaped model. Furthermore, the highest positive and negative pressure coefficients noticed on B surface were 0.68 and -0.68, respectively. These values were noticed on the vertical line from the 1 meter away from the corner. Also, the highest positive pressure coefficient on the C surface were noticed on the vertical line of 20 meter away from the re-entrant corner. The highest negative pressure coefficients were observed on vertical line 6-meter distance between the re-entrant corner. The highest positive and negative pressure coefficients on C surface are 0.69 and -0.81, respectively.

Moreover, the behavior of the pressure coefficients across the building height is similar to surfaces of L1 model.

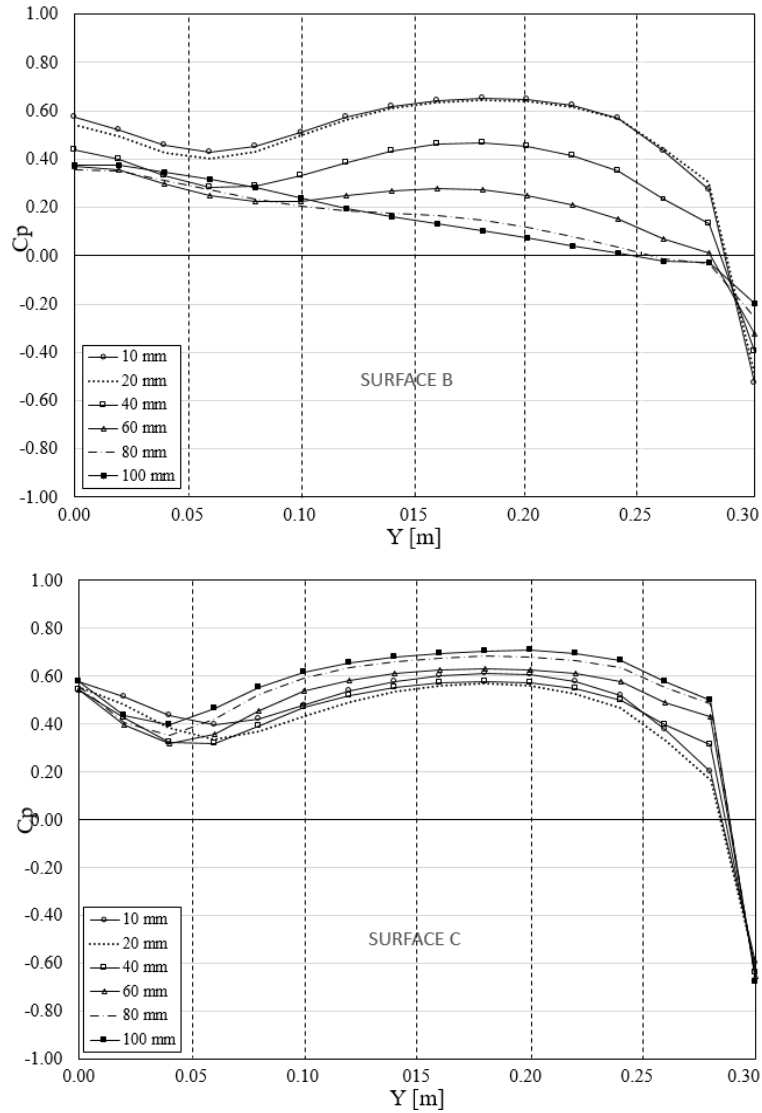


Figure 17. Pressure coefficients along the vertical lines of the L1 model for normal incident flow (0°) to surface B and surface C

The changes on pressure coefficient on the vertical lines designed at different distances from the corner of the building are shown in Figure 19 on the T1 formed models for the situation where the wind comes at an angle of 0° . On B surface, as the distance between vertical lines and re-entrant corner increase, the pressure coefficients decreased. Furthermore, the highest positive and negative pressure coefficients noticed on B surface were 0.19 and -0.15, respectively. These values were noticed on line 1 meter distance from the re-entrant corner. Pressure coefficients on all vertical lines on B surface of the T1 model showed similar behavior along the building height except the vertical lines which were distanced from 8 and 10 meter away from the re-entrant corner. At these vertical lines, the pressure coefficients showed sharp decreases along the height of the building. On the other hand, for T1 model, a regular

increase or decrease were not observed on the pressure coefficients on C surface related to the position of the vertical lines.

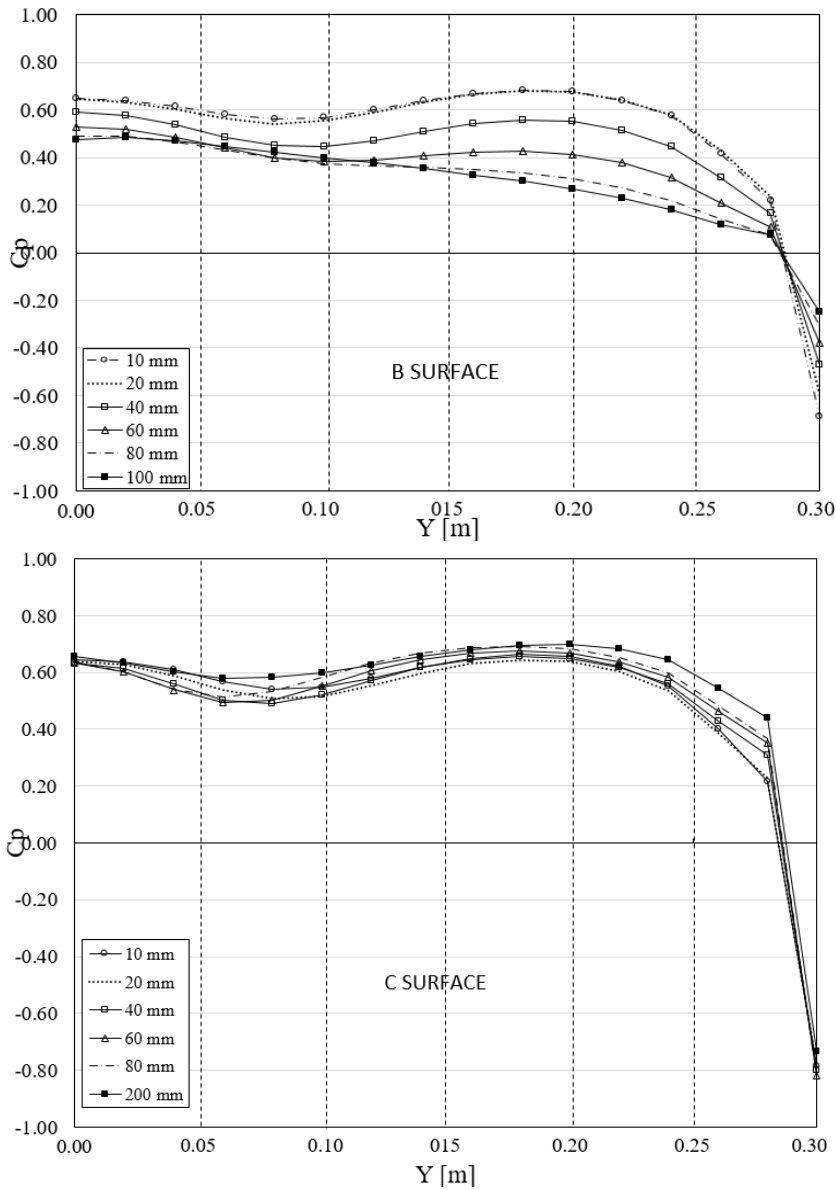


Figure 18. Pressure coefficients along the vertical lines of the L2 model for normal incident flow (0°) to surface B and surface C

The greatest positive pressure coefficients on the C surface were noticed on the vertical lines nearest to the middle of the C surface from 6-meter distance from the re-entrant corner and the highest negative pressure coefficients were observed on line distance of 1 meter from the re-entrant corner. The highest positive and negative pressure coefficients on C surface are 0.47 and -0.13, respectively. Furthermore, the pressure coefficients on all vertical lines increased approximately to 25 meters of the building height, then decrease and negative pressure coefficients were only observed on vertical lines away from 1 meter and 2 meter away from the re-entrant corners.

The changes on pressure coefficient on the vertical lines designed at different distances from the corner of the building are shown in Figure 20 on the T2 formed models for the situation where the wind comes at an

angle of 0° . On B surface, as the distance between vertical lines and re-entrant corner increase, the pressure coefficients decreased. Furthermore, the greatest positive and negative pressure coefficients noticed on B surface were 0.40 and -0.25, respectively.

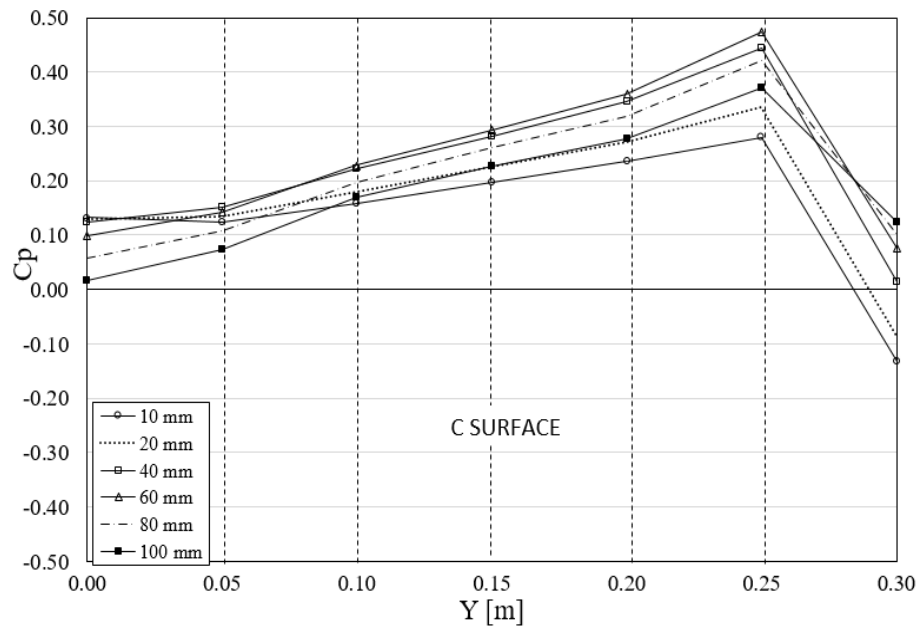
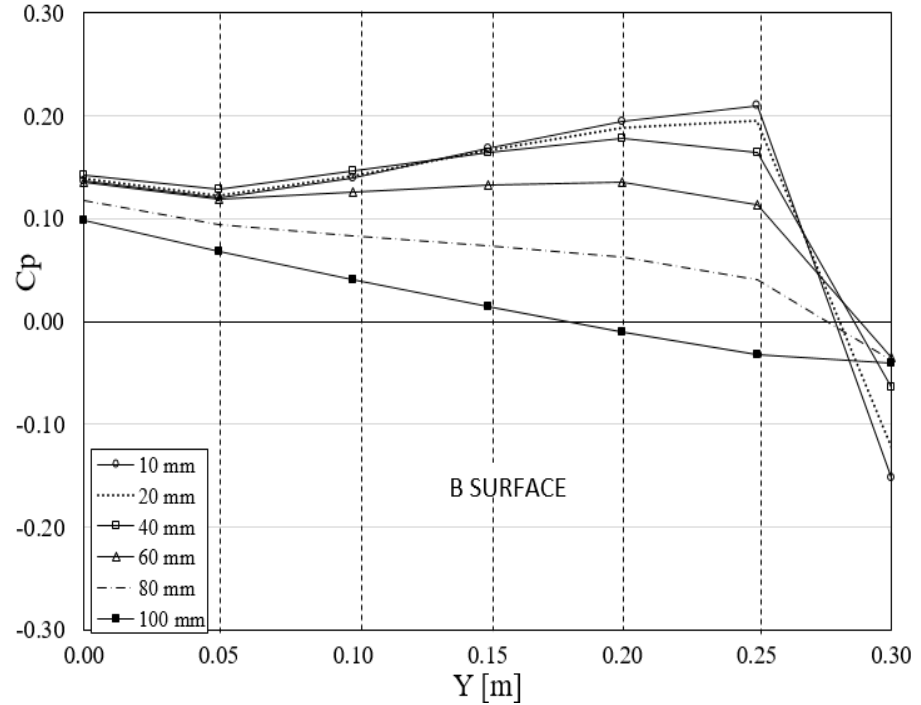


Figure 19. Pressure coefficients along the vertical lines of the T1 model for normal incident flow (0°) to surface B and surface C

These values were noticed on line 1-meter distance from the re-entrant corner. Pressure coefficients on all vertical lines on B surface of the T2 model showed similar behavior with T1 model along the building height except the vertical lines which were distanced from 8 and 10 meter away from the re-entrant corner. At these vertical lines, the pressure

coefficients showed sharp decreases along the height of the building. On the other hand, for T2 model pressure coefficients were generally increased on C surface, as the distance between vertical lines and re-entrant corner increase. Furthermore, the highest positive pressure coefficient on the C surface were noticed on line of 20-meter distance from the re-entrant corner.

The highest negative pressure coefficients were observed on vertical line 1 meter away from the re-entrant corner. The highest positive and negative pressure coefficients on C surface are 0.65 and -0.26, respectively. Furthermore, the pressure coefficients on all vertical lines decreased up to approximately 5 meters of the building height, then increased and again started to decrease from the 25-meter height level of the building.

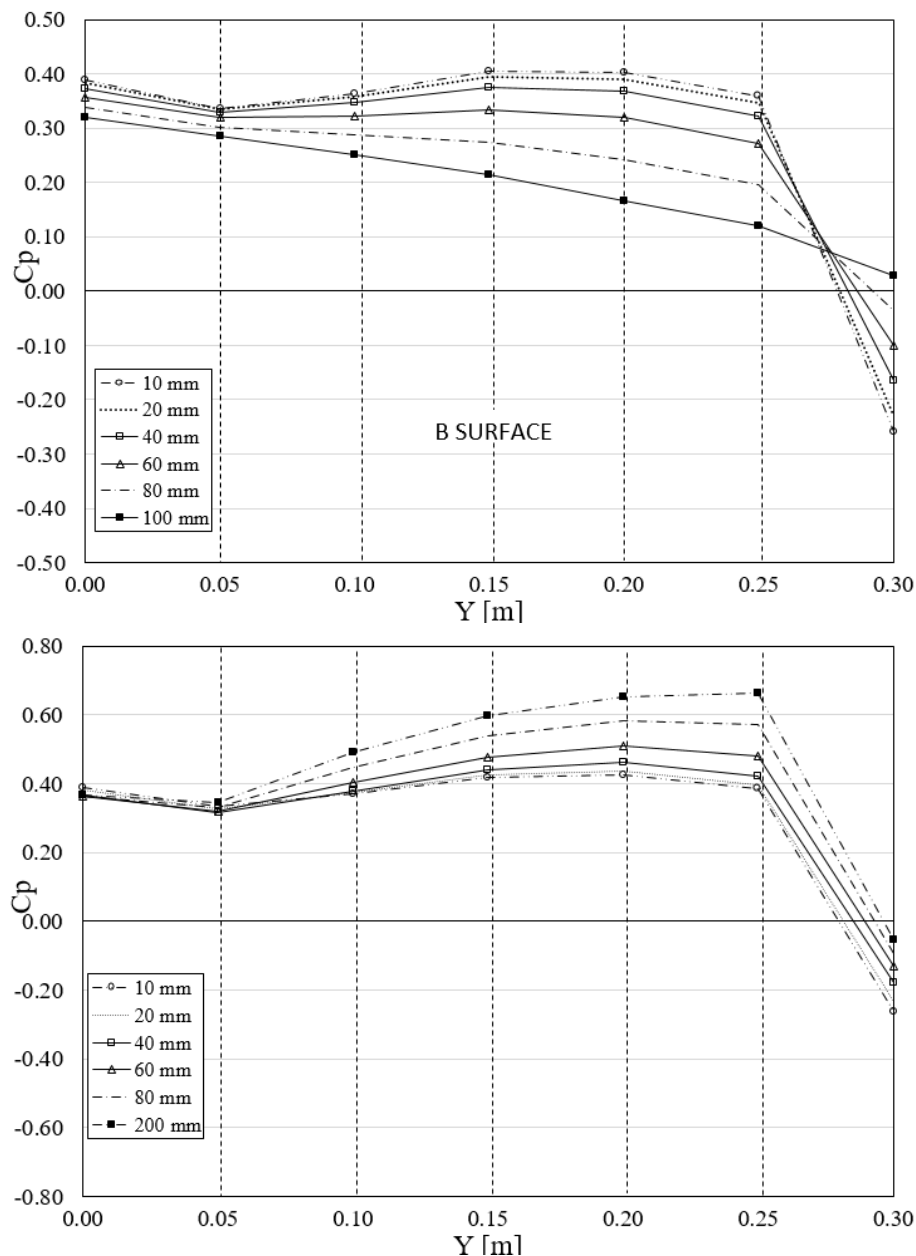


Figure 20. Pressure coefficients along the vertical lines of the T2 model for normal incident flow (0°) to surface B and surface C

Velocity Distributions

In Figures 21 (a) and 21 (b) the streamlines on mid-horizontal plane and on condition of 0° , and 180° wind angle, was given. Wind flows sharply at high velocity from the windward surface closest to the windward corners. The break and speed up of the flow noticed at the corners and the wind flow reverses just behind these corners, creating negative pressure regions. At 0° wind angle, two symmetrical eddies appear in the trace region of the T-formed building. It was like simple shaped buildings. However, solely a huge and unsymmetrical vortex appears behind the model at L Shaped building.

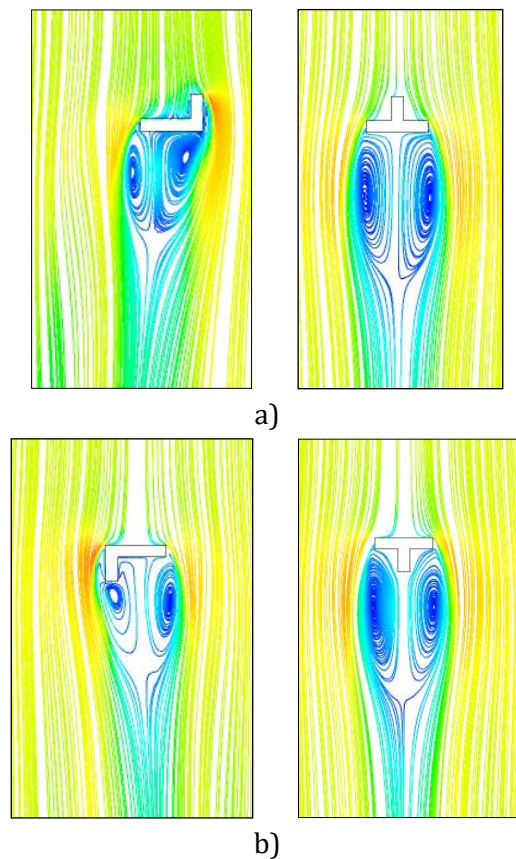


Figure 21. Streamlines around the L-shaped and T shaped model on the horizontal mid-plane ($H/2$), a) normal incident flow (0°) and b) 180° incident flow, respectively

When wind flow comes to the building the flow divided into two different areas as illustrated in Figures 22-24. Nearest to that areas, significant flows occur. The leeward surface of the model is usually wake area and smaller negative pressures is noticed. This causes drag forces in the leeward direction on surface of the building. The separated streams are reattached at the building's downwind rear stagnation point.

Wind flows around the different building forms were presented in Figures 22-24. On height level of $z=H/3$, turbulent flow is observed on the side surfaces of the all models. Moreover, the velocity in the track zone decreases and reverse flow zones are formed. The greatest velocity happens on side surfaces. It is observed that the maximum velocity region expanded with increasing height in all models for both wind incidence angle on the side surfaces. On the other hand, it is noticed that the drop

in the velocity in track area reduced with rising in height. At trace region, velocity decreases in all models in the velocity region. However, as the building height decreases, the velocity drops in track zone increases. Velocity region in L2 model is wider than L1 model. On the other hand, the velocity region at T2 models is larger than T1 models.

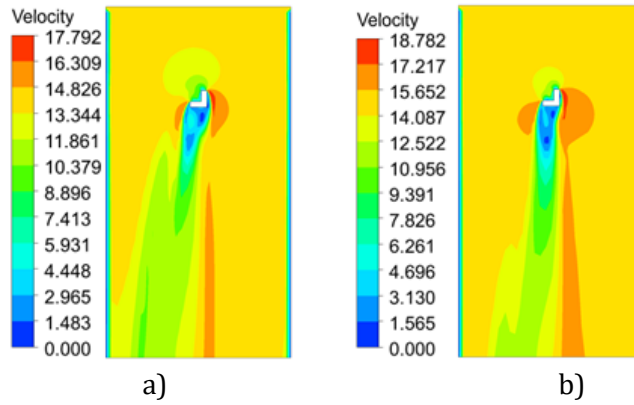
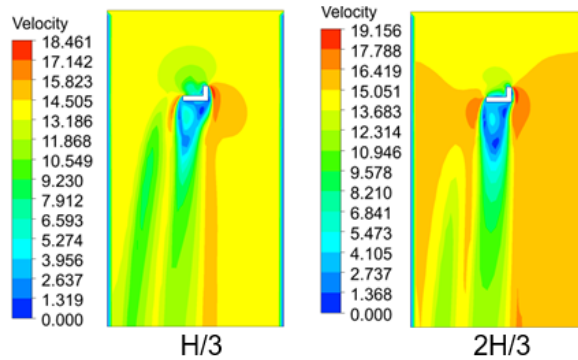
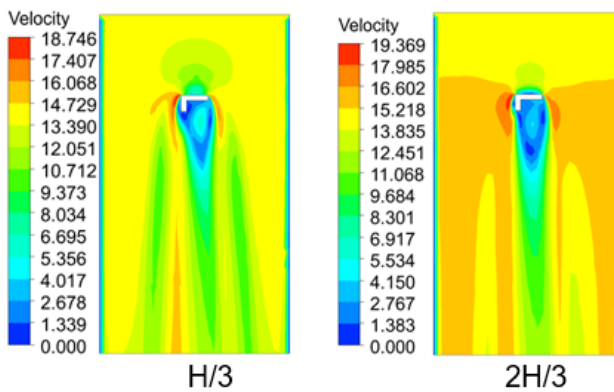


Figure 22. Velocity distributions around L1 model for normal incident flow (0°) a) $z=H/3$, b) $z=2H/3$, respectively



a)



b)

Figure 23. Velocity distributions around L2 model for $z=H/3$ and $2H/3$ level a) normal incident flow (0°) b) 180° incident flow, respectively

Figure 24. Velocity distributions around T1 model for normal incident flow (0°) a) $z=H/3$, b) $z=2H/3$, respectively

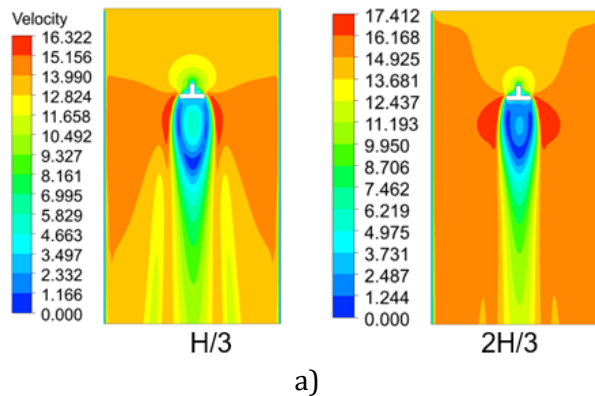
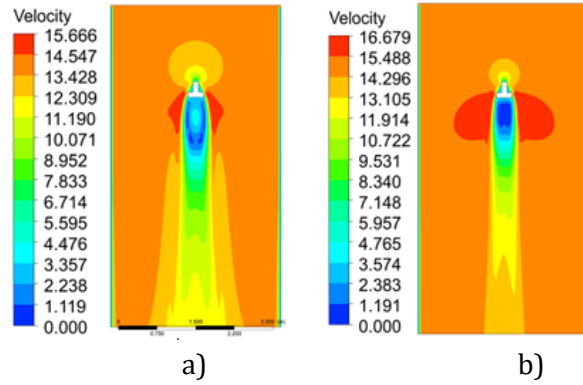
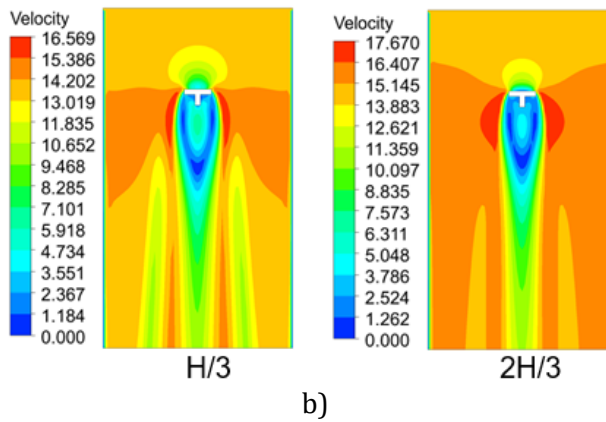


Figure 25. Velocity distributions around T2 model for $z=H/3$ and $2H/3$ level a) normal incident flow (0°) b) 180° incident flow, respectively



Conclusions

In this study, the variations on pressure coefficients for irregular formed buildings were analyzed for wind angles of 0° and 180° . The study aims to examine the significance of irregular plan shape, projection ratios, wind incidence angles, height levels, building areas and the re-entrant corner's distance on wind flow mechanism and variations on pressure distributions. L and T-shaped models which have similar building height but have dissimilar plan area and projections in plan were analyzed in detail. ANSYS Fluent 20.0 software is applied for analyzing the models. Flow is assumed as fully turbulent, steady and three dimensional. From analysis broad conclusions were obtained. As a result of the studies, it has been observed that the plan shape, wind incidence angle, projection

ratios of models, distances from the reentrant corner significantly affect the wind characteristics of models. The findings were evaluated based on projection ratios, wind incidence angles, building areas, the position of horizontal and vertical lines and wind flows.

If models were investigated according to the projection ratios and building areas, it was noticed that in L models while the increase in the projection ratio (PR) was considerably influence on positive and negative pressures. It was significantly observed in negative pressure coefficients. All pressure coefficients raise with the expansion of projection ratio (PR). On the other hand, it was noticed in all T models for the both wind incidence angles that while the positive pressure coefficients decrease with increase in the projection ratio and building area, negative pressure coefficients rise with the high projection ratios(PR). With the increase in building area, the highest negative pressures were seen in L2 and T2 models. When L and T models with the same building area are compared, the highest negative pressure was seen in the L model with a high PR (0.80). In L and T formed buildings, it was noticed that the negative pressure coefficients two times greater when the PR value decreased to half. In all T models, the greatest negative pressure coefficients were noticed on the D and F surfaces for both wind angles. In all L models, the greatest negative pressure coefficients were noticed on F surface for both wind angles.

When we looked at the pressure coefficients for building height level of $2H/3$, $H/2$ and $H/3$, it was observed that they increased related to building height's increase on all surfaces on all models for both 0° and 180° wind incidence angle. On the other hand, when we looked at the pressure coefficients on vertical lines which were replaced various distances from re-entrant corner, it was observed that the re-entrant corners distance significantly effects pressure coefficients. In general, it has been observed that the pressure values on the B surface decreased in all models, and increased on the C surface as moved away from the re-entrant corner.

When wind flows around the different building forms were examined, in all models, highest velocity occurs on side surfaces. It is observed that the maximum velocity region on side surfaces expanded with increasing height. In trace region, velocity decreases in all models. Wind is an important design parameter that should be considered from the initial stage of architectural design. This research intends to provide an awareness on buildings behavior exposing wind loads in order to create solutions for different conditions on each part of architectural design phase especially architects and architectural students The obtained results from the CFD analysis will supply extensive data about the wind load effects on irregular buildings.

ACKNOWLEDGEMENTS/NOTES

The author thanks to Assist. Prof.Dr. İlknur Acar Ata for her moral and support during the evaluation process of the study.

CONFLICT OF INTEREST

No conflict of interest was declared by the author.

FINANCIAL DISCLOSURE

The author declared that this study has received no financial support.

ETHICS COMMITTEE APPROVAL

Ethics committee approval was not required for this article.

LEGAL PUBLIC/PRIVATE PERMISSIONS

There was not required any permission for this article.

REFERENCES

Ahmad, S., & Kumar, K. (2002). Effect of geometry on wind pressures on low-rise hip roof buildings. *Journal of Wind Engineering and Industrial Aerodynamics*, 90(7), 755-779.

Al-Najjar, S. F., & Al-Azhari, W. W. (2021). Review of Aerodynamic Design Configurations for Wind Mitigation in High-Rise Buildings: Two Cases from Amman. *International Journal of Performability Engineering*, 17(4).

Bairagi, A. K., & Dalui, S. K. (2020). Distribution of wind pressure around different shape tall building *Advances in Structures, Systems and Materials* (pp. 31-38): Springer, Singapore.

Bandi, E. K., Tamura, Y., Yoshida, A., Kim, Y. C., & Yang, Q. (2013). Experimental investigation on aerodynamic characteristics of various triangular-section high-rise buildings. *Journal of Wind Engineering and Industrial Aerodynamics*, 122, 60-68.

Behera, S., Ghosh, D., Mittal, A. K., Tamura, Y., & Kim, W. (2020). The effect of plan ratios on wind interference of two tall buildings. *The Structural Design of Tall and Special Buildings*, 29(1).

Bhattacharyya, B., & Dalui, S. K. (2018). Investigation of mean wind pressures on 'E'plan shaped tall building. *Wind and structures*, 26(2), 99-114.

Bhattacharyya, B., & Dalui, S. K. (2020). Experimental and numerical study of wind-pressure distribution on irregular-plan-shaped building. *Journal of Structural Engineering*, 146(7).

Bhattacharyya, B., Dalui, S. K., & Ahuja, A. K. (2014). Wind induced pressure on 'E'plan shaped tall buildings. *Jordan J Civ Eng*, 8, 120-134.

Blocken, B., Carmeliet, J., & Stathopoulos, T. (2007). CFD evaluation of wind speed conditions in passages between parallel buildings—effect of wall-function roughness modifications for the atmospheric boundary layer flow. *Journal of Wind Engineering and Industrial Aerodynamics*, 95(9-11), 941-962.

Chakraborty, S., Dalui, S. K., & Ahuja, A. K. (2014). Wind load on irregular plan shaped tall building-a case study. *Wind and structures*, 19(1), 59-73.

Chen, B., Cheng, W., Ma, H., & Yang, Q. (2021). Wind interference effects from one high-rise building and similar low-rise flat-roof buildings. *Journal of Structural Engineering*, 147(9).

Franke, J. (2006). *Recommendations of the COST action C14 on the use of CFD in predicting pedestrian wind environment*. Paper presented at the The fourth international symposium on computational wind engineering, Yokohama, Japan.

Gomes, M. G., Rodrigues, A. M., & Mendes, P. (2005). Experimental and numerical study of wind pressures on irregular-plan shapes. *Journal of Wind Engineering and Industrial Aerodynamics*, 93(10), 741-756.

He, B.-J., Yang, L., & Ye, M. (2014). Strategies for creating good wind environment around Chinese residences. *Sustainable Cities and Society*, 10, 174-183.

He, Y., Liang, Q., Li, Z., Fu, J., Wu, J., & Deng, T. (2019). Accurate estimation of tube-induced distortion effects on wind pressure measurements. *Journal of Wind Engineering and Industrial Aerodynamics*, 188, 260-268.

Hu, G., Song, J., Hassanli, S., Ong, R., & Kwok, K. C. (2019). The effects of a double-skin façade on the cladding pressure around a tall building. *Journal of Wind Engineering and Industrial Aerodynamics*, 191, 239-251.

Huang, P., Luo, P., & Gu, M. (2005). *Pressure and forces measurements on CAARC standard Tall building in wind tunnel of Tong Ji University*. Paper presented at the Proceedings of the 12th national wind engineering conference of China, Xi'an, China.

Jendzelovsky, N., & Antal, R. (2021). CFD and Experimental Study of Wind Pressure Distribution on the High-Rise Building in the Shape of an Equilateral Acute Triangle. *Fluids*, 6(2), 81.

Kummitha, O. R., Kumar, R. V., & Krishna, V. M. (2021). CFD analysis for airflow distribution of a conventional building plan for different wind directions. *Journal of Computational Design and Engineering*, 8(2), 559-569.

Kushal, T., Ahuja, A., & Chakrabarti, A. (2013). An experimental investigation of wind pressure developed in tall buildings for different plan shape. *Int J Innov Res Studies*, 1(12), 605-614.

Li, Y., Duan, R.-B., Li, Q.-S., Li, Y.-G., & Li, C. (2020). Research on the characteristics of wind pressures on L-shaped tall buildings. *Advances in Structural Engineering*, 23(10), 2070-2085.

Liu, Z., Yu, Z., Chen, X., Cao, R., & Zhu, F. (2020). An investigation on external airflow around low-rise building with various roof types: PIV measurements and LES simulations. *Building and Environment*, 169.

Mallick, M., Kumar, A., & Patra, K. C. (2019). Experimental investigation on the wind-induced pressures on C-shaped buildings. *KSCE Journal of Civil Engineering*, 23(8), 3535-3546.

Mallick, M., Mohanta, A., Kumar, A., & Patra, K. C. (2020). *Gene-expression programming for the assessment of surface mean pressure coefficient on building surfaces*. Paper presented at the Building Simulation.

Mou, B., He, B.-J., Zhao, D.-X., & Chau, K.-w. (2017). Numerical simulation of the effects of building dimensional variation on wind pressure distribution. *Engineering Applications of Computational Fluid Mechanics*, 11(1), 293-309.

- Mukherjee, S., Chakraborty, S., Dalui, S. K., & Ahuja, A. K. (2014). Wind induced pressure on 'Y' plan shape tall building. *Wind & structures*, 19(5), 523-540.
- Pal, S., Raj, R., & Anbukumar, S. (2021). Comparative study of wind induced mutual interference effects on square and fish-plan shape tall buildings. *Sādhanā*, 46(2), 1-27.
- Paul, R., & Dalui, S. (2021). Shape Optimization to Reduce Wind Pressure on the Surfaces of a Rectangular Building with Horizontal Limbs. *Periodica Polytechnica Civil Engineering*, 65(1), 134-149.
- Peng, H., Dai, S., Lin, K., Hu, G., & Liu, H. (2020). Experimental investigation of wind characteristics and wind energy potential over rooftops: Effects of building parameters. *Journal of Wind Engineering and Industrial Aerodynamics*, 205.
- R.Kar, & Dalui, S. K. (2016). Wind interference effect on an octagonal plan shaped tall building due to square plan shaped tall buildings. *International Journal of Advanced Structural Engineering (IJASE)*, 8(1), 73-86.
- Sanyal, P., & Dalui, S. K. (2020). Comparison of aerodynamic coefficients of various types of Y-plan-shaped tall buildings. *Asian Journal of Civil Engineering*, 21, 1109-1127.
- Sanyal, P., & Dalui, S. K. (2021). Effects of internal angle between limbs of "Y" plan shaped tall building under wind load. *Journal of Building Engineering*, 33.
- Sy, L. D., Yamada, H., & Katsuchi, H. (2019). Interference effects of wind-over-top flow on high-rise buildings. *Journal of Wind Engineering and Industrial Aerodynamics*, 187, 85-96.
- Tanaka, H., Tamura, Y., Ohtake, K., Nakai, M., & Kim, Y. C. (2012). Experimental investigation of aerodynamic forces and wind pressures acting on tall buildings with various unconventional configurations. *Journal of Wind Engineering and Industrial Aerodynamics*, 107, 179-191.
- Tominaga, Y., Mochida, A., Yoshie, R., Kataoka, H., Nozu, T., Yoshikawa, M., & Shirasawa, T. (2008). AIJ guidelines for practical applications of CFD to pedestrian wind environment around buildings. *Journal of Wind Engineering and Industrial Aerodynamics*, 96(10-11), 1749-1761.
- Tse, K. T., Chen, Z.-S., Lee, D.-E., & Kim, B. (2021). Effect of aerodynamic modifications on the surface pressure patterns of buildings using proper orthogonal decomposition. *Wind and structures*, 32(3), 227-238.
- Verma, S., Ahuja, A., & Pandey, A. (2013). Effects of wind incidence angle on wind pressure distribution on square pan tall buildings. *Journal of Academic Industrial Research*, 1(12), 747-752.
- Weerasuriya, A. (2013). Computational Fluid Dynamic (CFD) simulation of flow around tall buildings. *Engineer: Journal of the Institution of Engineers, Sri Lanka*, 46(3).
- Xu, X., Yang, Q., Yoshida, A., & Tamura, Y. (2017). Characteristics of pedestrian-level wind around super-tall buildings with various configurations. *Journal of Wind Engineering and Industrial Aerodynamics*, 166, 61-73.



Zhao, D.-X., & He, B.-J. (2017). Effects of architectural shapes on surface wind pressure distribution: case studies of oval-shaped tall buildings. *Journal of Building Engineering*, 12, 219-228.

Zhou, L., Tse, K. T., Hu, G., & Li, Y. (2021). Mode interpretation of interference effects between tall buildings in tandem and side-by-side arrangement with POD and ICA. *Engineering Structures*, 243, 112616.

Resume

Tuğba İnan Günaydın currently works at Niğde Ömer Halisdemir University, Department of Architecture, as an assistant prof. She received her M.Arch and ph.d in architecture from İzmir Institute of Technology. She has been studying on energy performance, wind flow analysis, double skin façade systems, building science and technology, earthquake resistant design.